NATIONAL TRANSPORTATION SAFETY BOARD
Office of Research and Engineering
Materials Laboratory Division
Washington, D.C. 20594

September 2, 2020

MATERIALS LABORATORY FACTUAL REPORT Report No. 20-038

1. ACCIDENT INFORMATION

Place	:	Big Timber, Montana
Date	:	January 16, 2020
Vehicle	:	Cessna 172Q, N96145
NTSB No.	:	WPR20LA068
Investigator	:	Stephen Stein, AS-WPR

2. COMPONENTS EXAMINED

Remnants of a propeller blade assembly

3. DETAILS OF THE EXAMINATION

On January 16, 2020, about 2000 mountain standard time, a Cessna 172Q airplane was substantially damaged when it impacted the ground following a total loss of engine power near Big Timber Airport in Big Timber, MT. The flight instructor and student pilot were not injured. According to a diagram furnished by the instructor, the airplane impacted the ground about 425 yards northwest of the runway and slid about 125 yards before it came to rest. The instructor located an approximately 1-foot long section of a blade tip in the debris path. The airplane was retained for further examination, and the remnants of the propeller blade assembly were sent to the NTSB Materials Laboratory in Washington, DC.

Figure 1 and Figure 2 shows the propeller assembly remnants, as received. The propeller was submitted with the hub attachment still affixed. The blade assembly had fractured in two places, one at the very tip, shown in right in Figure 1, and the other approximately 10 inches from the tip. This second remnant was reported found away from the debris field.

Figure 3 shows a closer view of the aft hub attachment, highlighting the bolt holes. There were no indications of damage on the aft face, as shown in the figure. The bolt holes did not exhibit any indications of chatter or fretting, nor other damage such as cracking or plastic deformation on the interior or exterior surfaces.

As demonstrated in Figure 2, the propeller exhibited plastic deformation on both blades. The deformation was oriented from the forward to aft faces of the propeller,

consistent with impact with either the ground or ground-based objects while still moving forward. Figure 4 shows the intact blade side, shown from the fractured tip. The leading edge surfaces of the blade presented the exposed underlying aluminum metal, consistent with missing black paint (the propeller blade had been painted black, with the tips painted as white stripes). These regions contained scratches and deep gouges, all of which were oriented parallel to the chord line. At the tip shown in Figure 4, these gouges were most pronounced, and were located near where the tip had fractured. The tip was bent upward adjacent to the fracture, as depicted in Figure 4.

Examination of this fractured tip revealed the fracture surface exhibited a general slant orientation, with characteristics consistent with that of cupping or a U-shape. The surface was jagged in appearance, with rough features. The surface exhibited a dull luster with fibrous features. These characteristics were consistent with overstress fracture of this blade tip in bending and torsion.

Figure 5 shows the fractured remnant of the opposite blade, which had been found separate. This remnant exhibited areas of missing paint, located along the leading edge and adjacent to the inboard fracture surface. The missing paint on the leading edge was co-located with parallel scratches, which were oriented at a 45° angle towards the outboard direction, running towards the trailing edge. Figure 6 shows the blade remnant fracture surface side. The remnant exhibited plastic deformation on the outboard tip surfaces, exhibiting curling or twisting from the leading edge towards the trailing edge.

A closer view of the remnant fracture surface is illustrated in Figure 7 and Figure 8. The leading edge exhibited repeating concentric features that were oriented convex appearance toward the leading edge. This portion of the fracture surface exhibited areas of rough, dull textures, along with areas that were more reflective. The reflective areas were consistent with metallic smearing, due to post-fracture wear and impact damage. The trailing edge portion exhibited a jog approximately 1.75 inches from the edge (Figure 8). Aft of the jog, the blade remnant twisted upward in the figure, consistent with plastic deformation from torsional stresses. The aftmost portion of the fracture surface exhibited enough smearing to render it visually featureless.

Due to the amount of post-fracture damage, the mating inboard face of the remnant fracture surface (on the main propeller assembly) was sectioned and then cleaned with acetone to facilitate additional examination (shown in Figure 9). The entire fracture surface was examined using a scanning electron microscope (SEM). Figure 10, Figure 11, and Figure 12 show typical areas of the blade fracture surface from the leading edge, midpoint, and trailing edge, respectively. As shown in all the micrographs, the fracture surface exhibited dimpled rupture, consistent with fracture from overstress. There were no indications of pre-existing fracture modes, such as striations or intergranular fracture. Multiple areas along the fracture surface did exhibit streaks and gouges, oriented in an erratic pattern. These features were consistent with damage such as smearing from post-fracture impact and rubbing.

The tip of the intact but bent propeller blade (Figure 4) and the tip of the fractured blade remnant (left in Figure 5) were sectioned and examined using a SEM. Figure 13 and Figure 14 shows typical areas of the opposite propeller blade tip from the trailing and leading edges, respectively. These areas exhibited dimpled rupture, consistent with overstress fracture. Figure 15 and Figure 16 show typical areas of the tip of the fractured remnant, from the leading and trailing edges, respectively. Likewise, these areas exhibited dimpled rupture, consistent with overstress fracture. However, most of fractured surfaces of both tips exhibited smearing and gouging, consistent with post-fracture damage. Figure 17 shows a typical example of this smearing damage, which was inconsistent with any pre-existing failure mode.

A small portion of the propeller blade material was backcut and intentionally overstressed (laboratory broken) to simulate an overstress fracture. Figure 18 and Figure 19 show typical examples of this laboratory-fractured material. The fractures exhibited dimpled rupture. These fracture features were comparable with those observed on all the examined propeller fracture surfaces.

The chemical composition of the sectioned propeller fragment was examined using x-ray fluorescence (XRF) and energy dispersive x-ray spectroscopy (EDS). From the data obtained using these techniques, the propeller was found to be consistent with AA 2014 aluminum alloy. The electrical conductivity of the spar was examined per ASTM E1004.[1] The conductivity averaged 36.8 %IACS. The hardness was inspected per ASTM E18.[2] The hardness averaged 71 HRBW. Per AMS 2658, these data were consistent with an AA 2014 alloy in a T3 or T4 temper.[3,4]

Erik M Mueller
Materials Research Engineer

[1] ASTM E1004 – *Standard Test Method for Determining Electrical Conductivity Using the Electromagnetic (Eddy-Current) Method.* ASTM International, West Conshohocken, PA

[2] ASTM E18 – *Standard Test Methods for Rockwell Hardness and Rockwell Superficial Hardness of Metallic Materials*. ASTM International, West Conshohocken, PA.

[3] AMS 2658 – *Hardness and Conductivity Inspection of Wrought Aluminum Alloy Parts*. SAE International, Warrendale, PA.

[4] AA 2014 is a common aluminum alloy strengthened by precipitation hardening from the Cu, Mn, and Mg alloying elements. The T3 and T4 temper is the heat treatment prescribed for solutioning and then coldworking or natural aging, respectively.

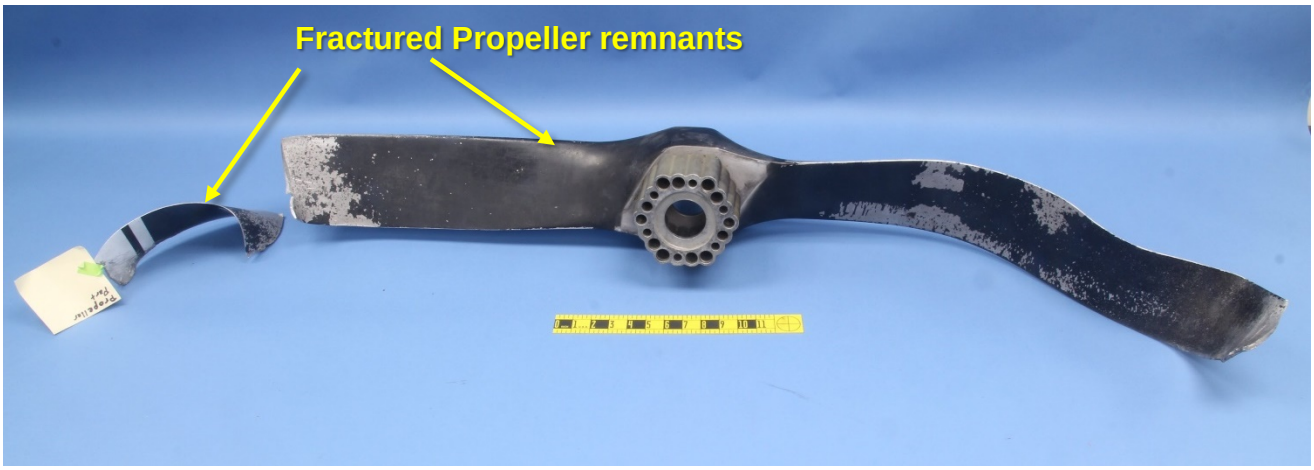

Figure 1 – The propeller and the hub remnants, viewed from the aft or engine-facing side.

Figure 2 – The propeller remnants viewed from the forward side, opposite that in Figure 1.

Figure 3 – View of the propeller hub attachment, viewed from the aft face.

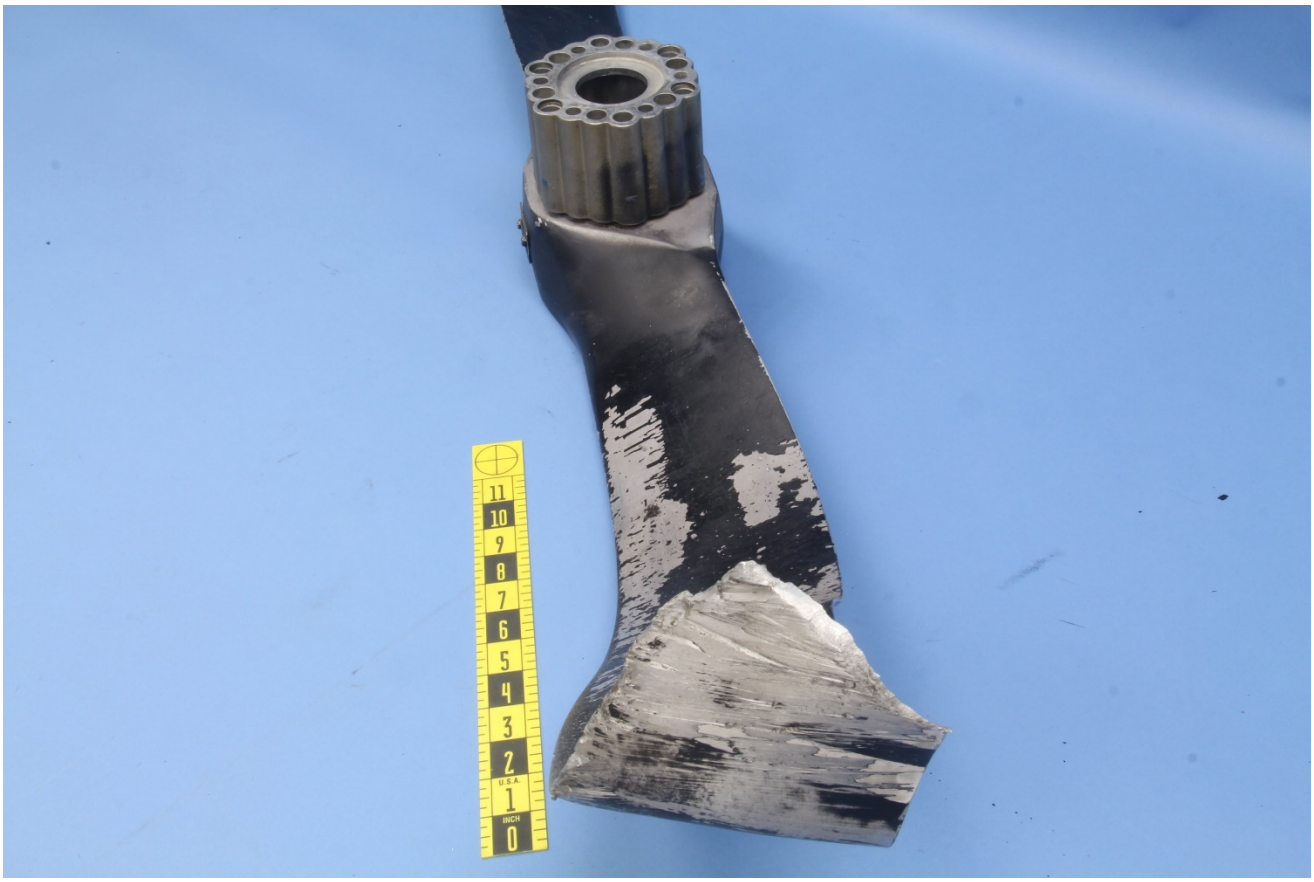

Figure 4 – View of the bent and fractured tip of the intact blade side, as received.

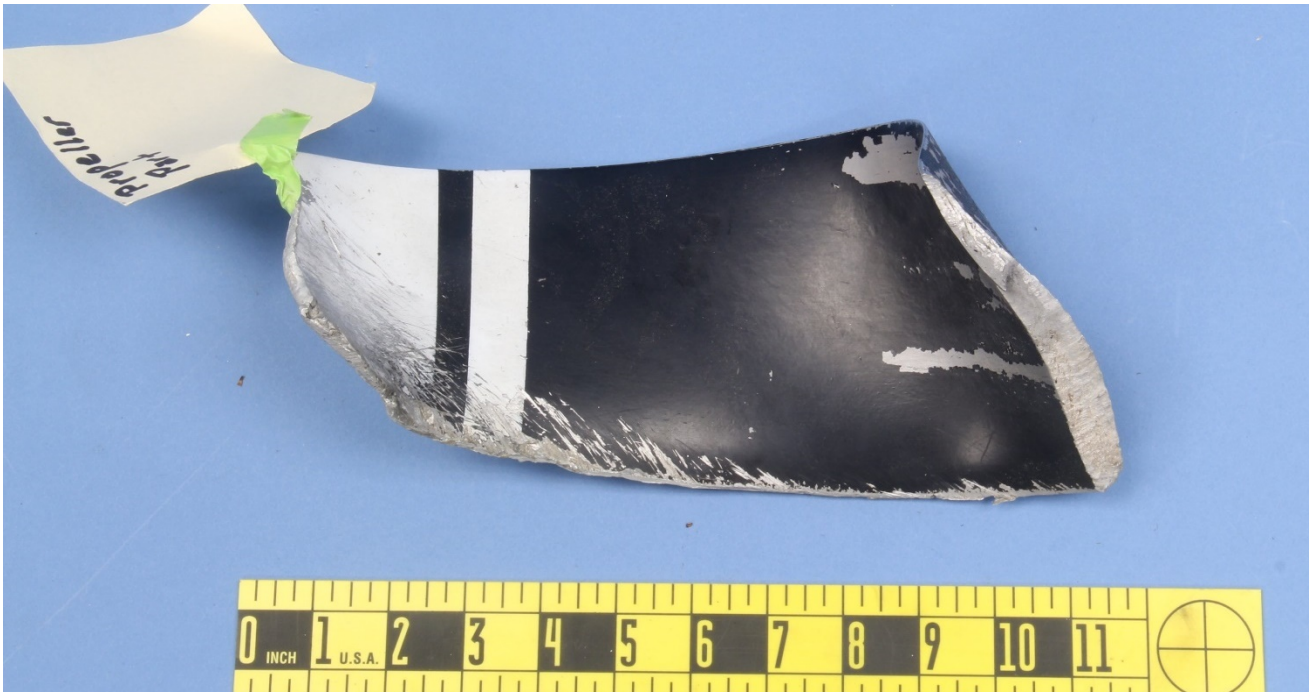

Figure 5 – View of the fractured blade side remnant found away from the debris field.

Figure 6 – View of the fracture surface from the blade remnant.

Figure 7 – Closer view of the leading edge of the blade fracture surface remnant.

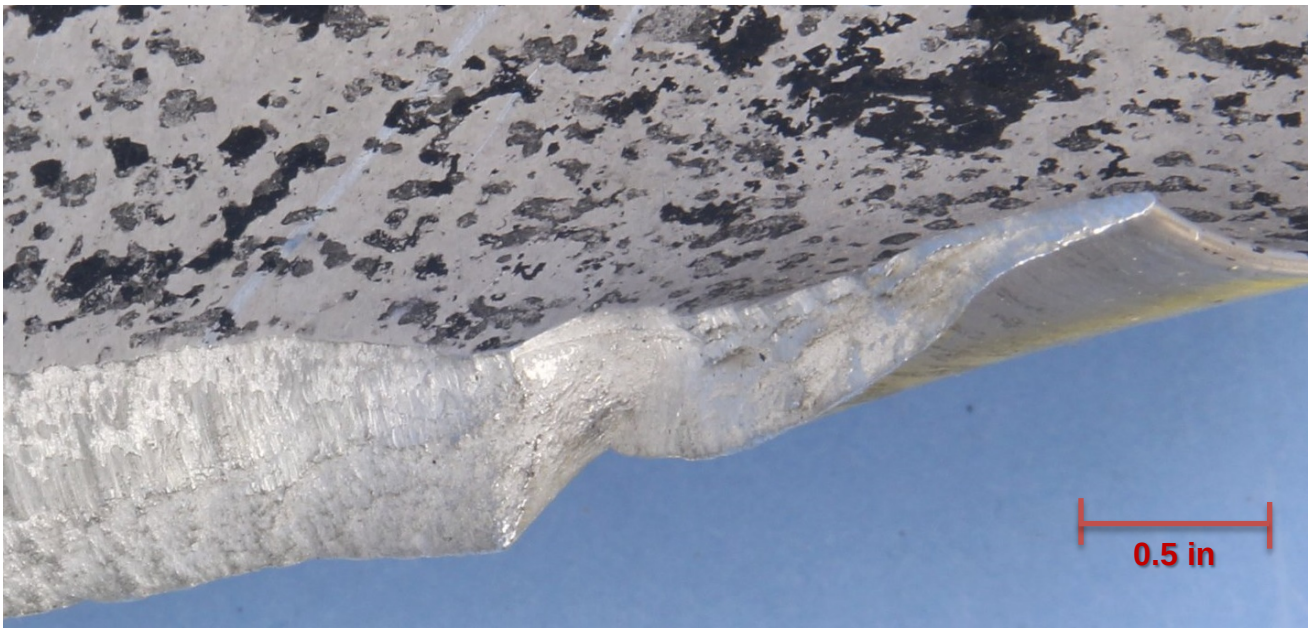

Figure 8 – Closer view of the trailing edge of the fracture surface of the propeller remnant.


Figure 9 – The mating inner fracture surface of the fractured propeller blade, viewed after sectioning and cleaning.

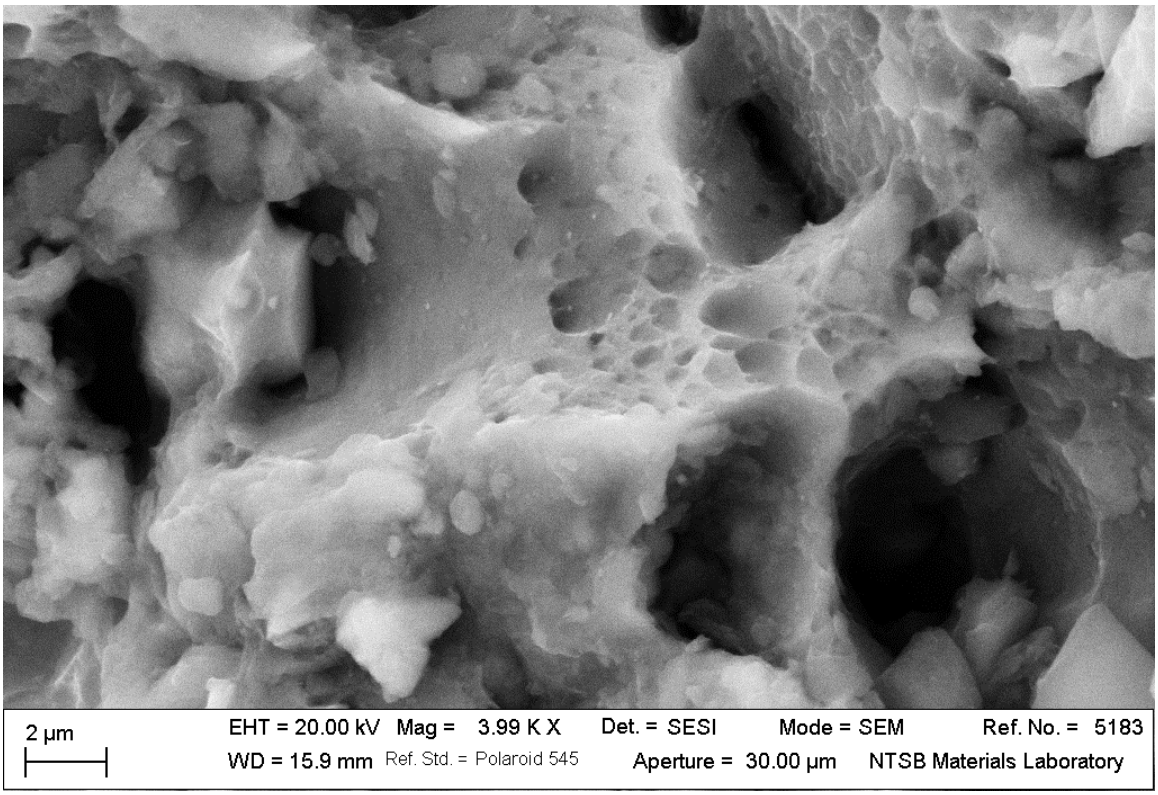

Figure 10 – Secondary electron (SE) micrograph of an area of the fracture surface near the leading edge, showing dimpled rupture.

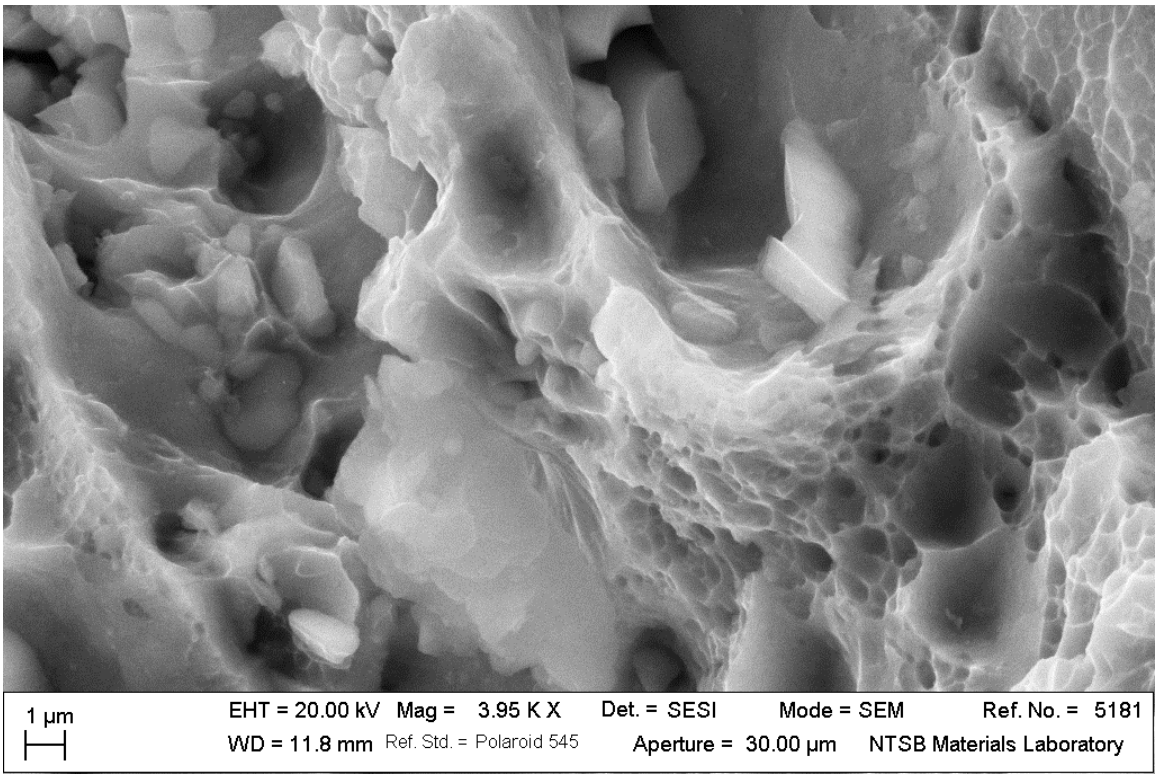

Figure 11 – SE micrograph of an area in the middle of the fracture surface, showing dimpled rupture.

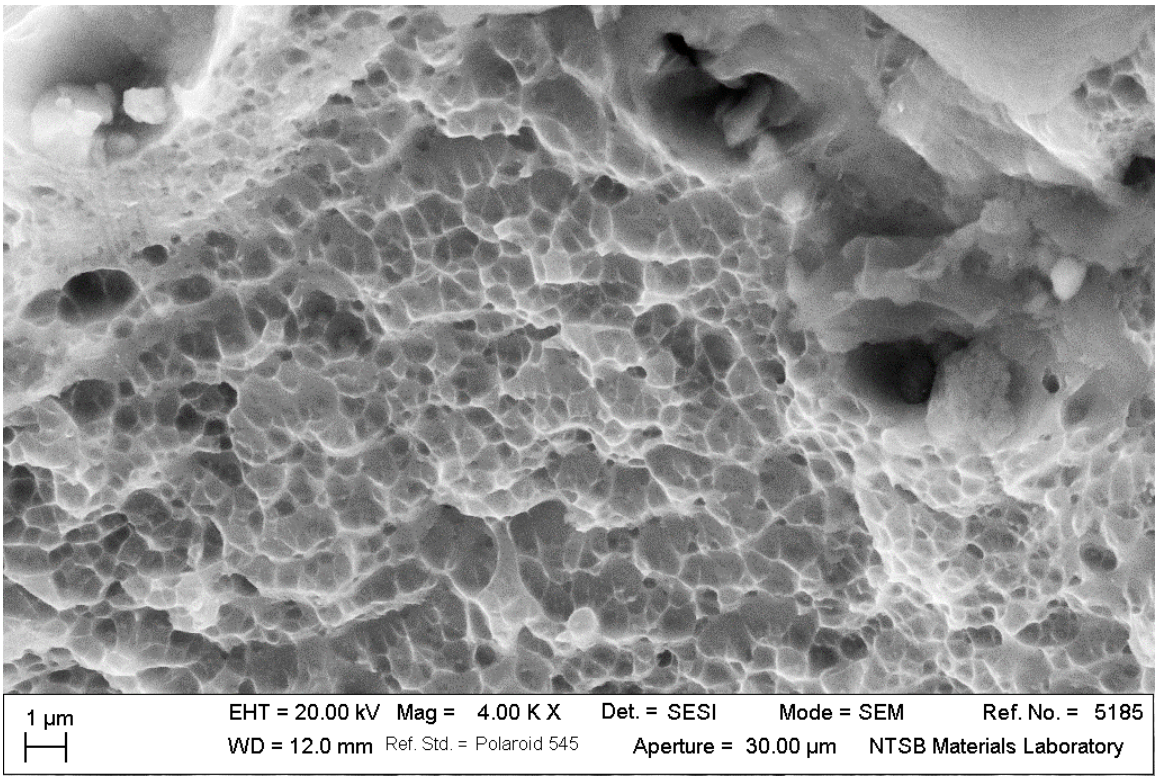

Figure 12 – SE micrograph of dimpled rupture on the fracture surface near the trailing edge.

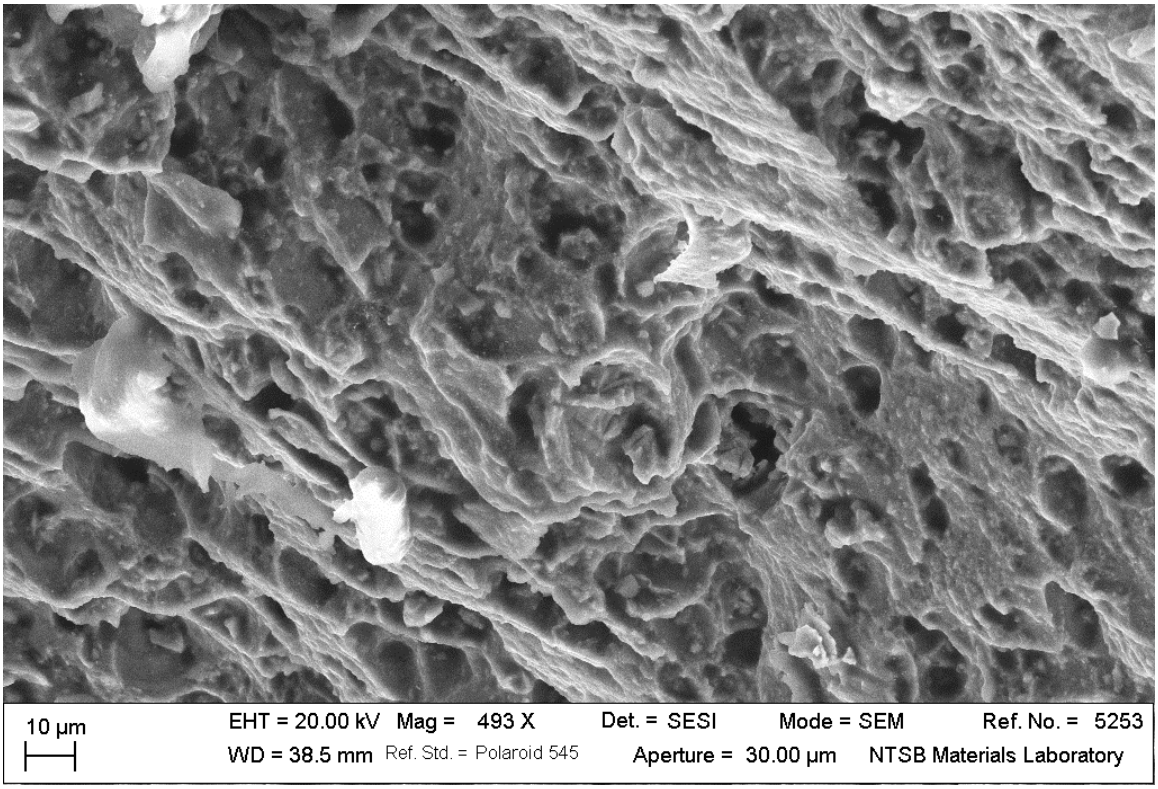

Figure 13 – SE micrograph of dimpled rupture near the trailing edge of the unbroken opposite blade tip.

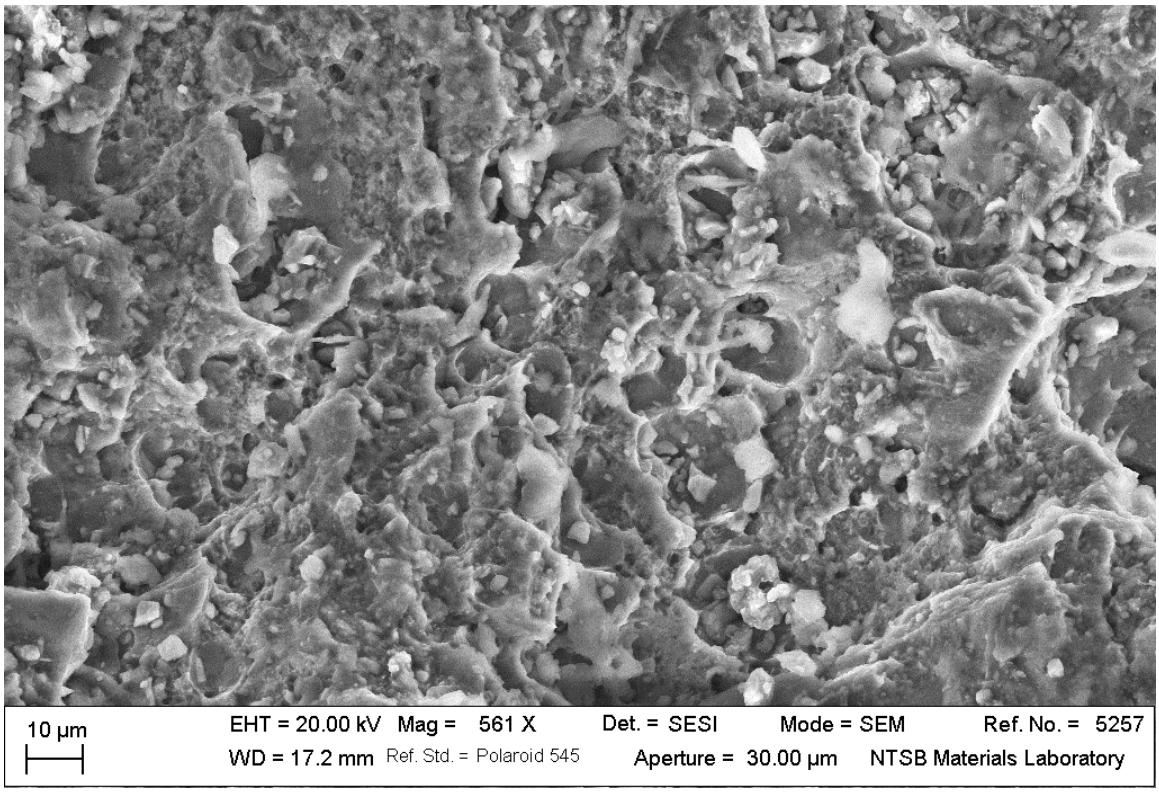

Figure 14 – SE micrograph of dimpled rupture near the leading edge of the unbroken opposite blade tip.

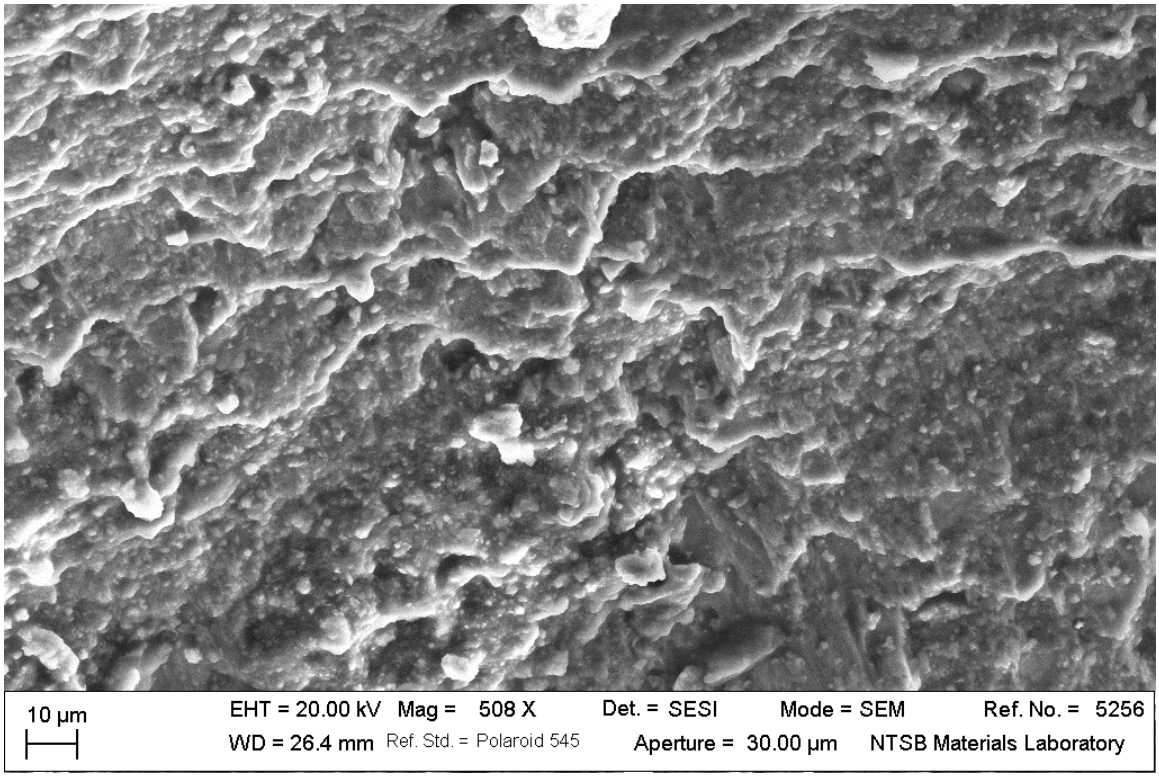

Figure 15 – SE micrograph of dimpled rupture on the leading edge of the remnant piece tip.

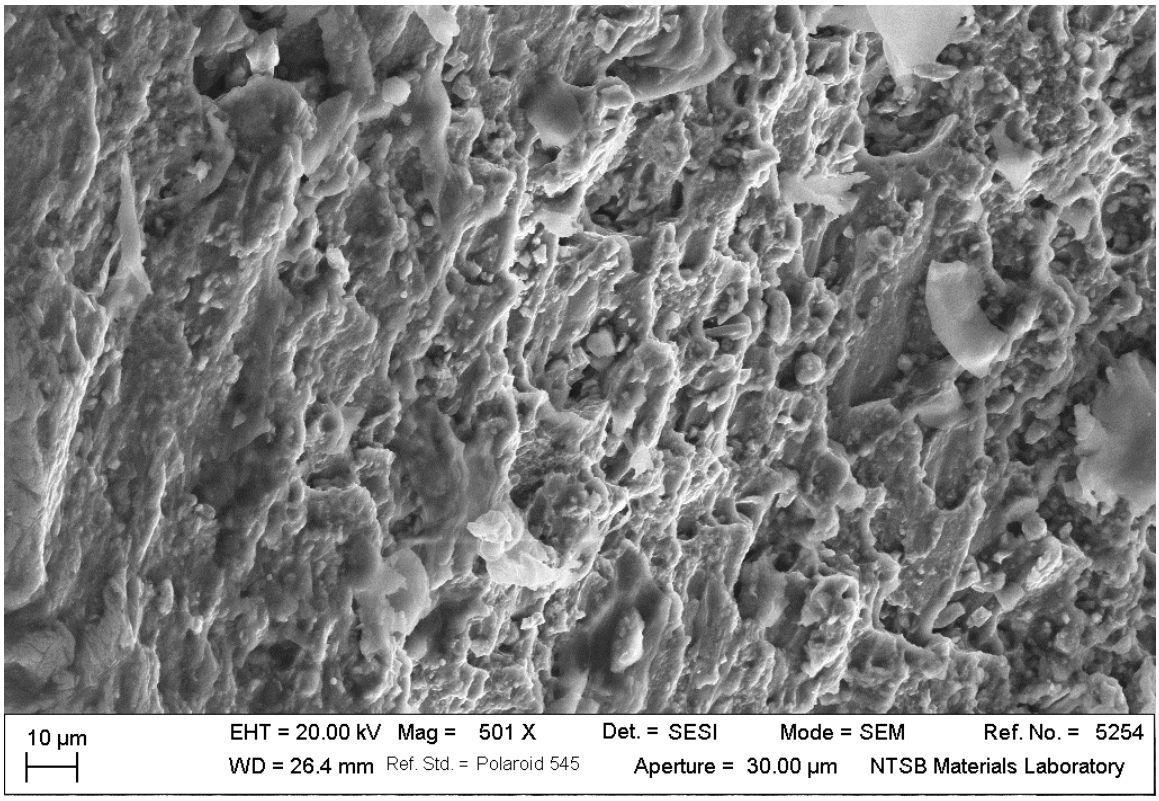

Figure 16 – SE micrograph of dimpled rupture on the trailing edge of the remnant piece tip.

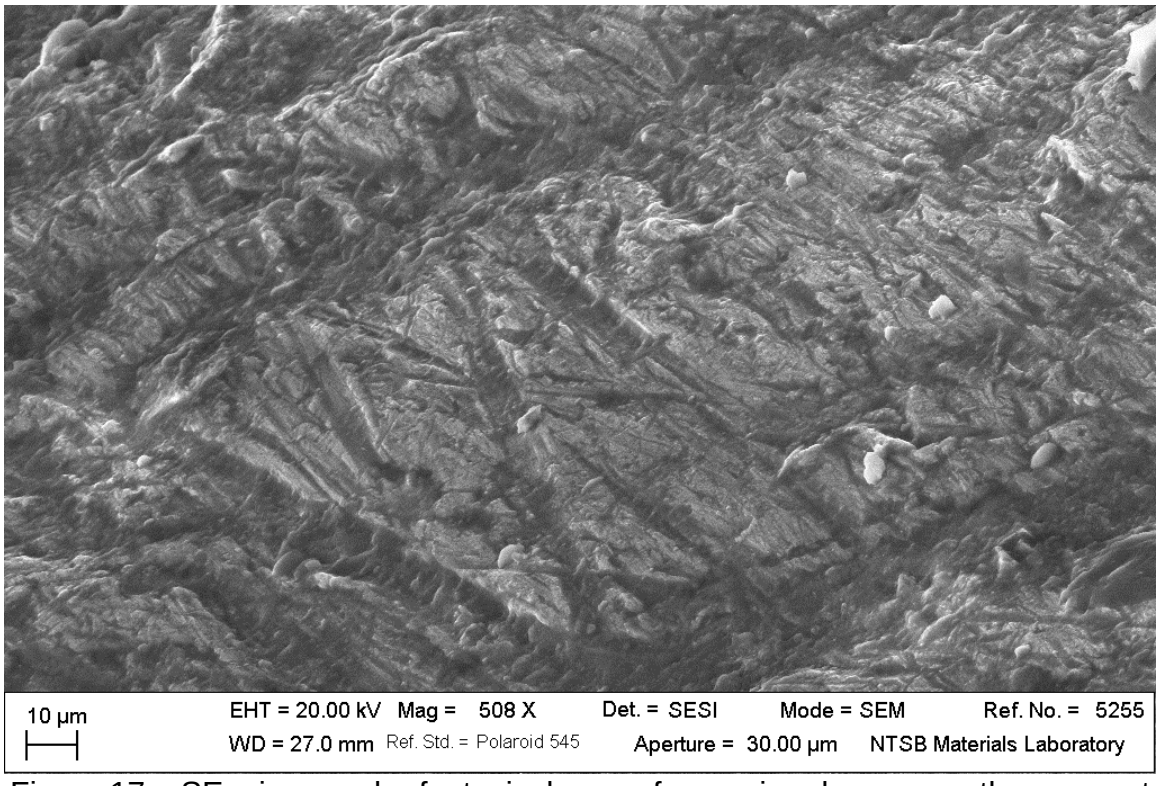

Figure 17 – SE micrograph of a typical area of smearing damage on the remnant tip.

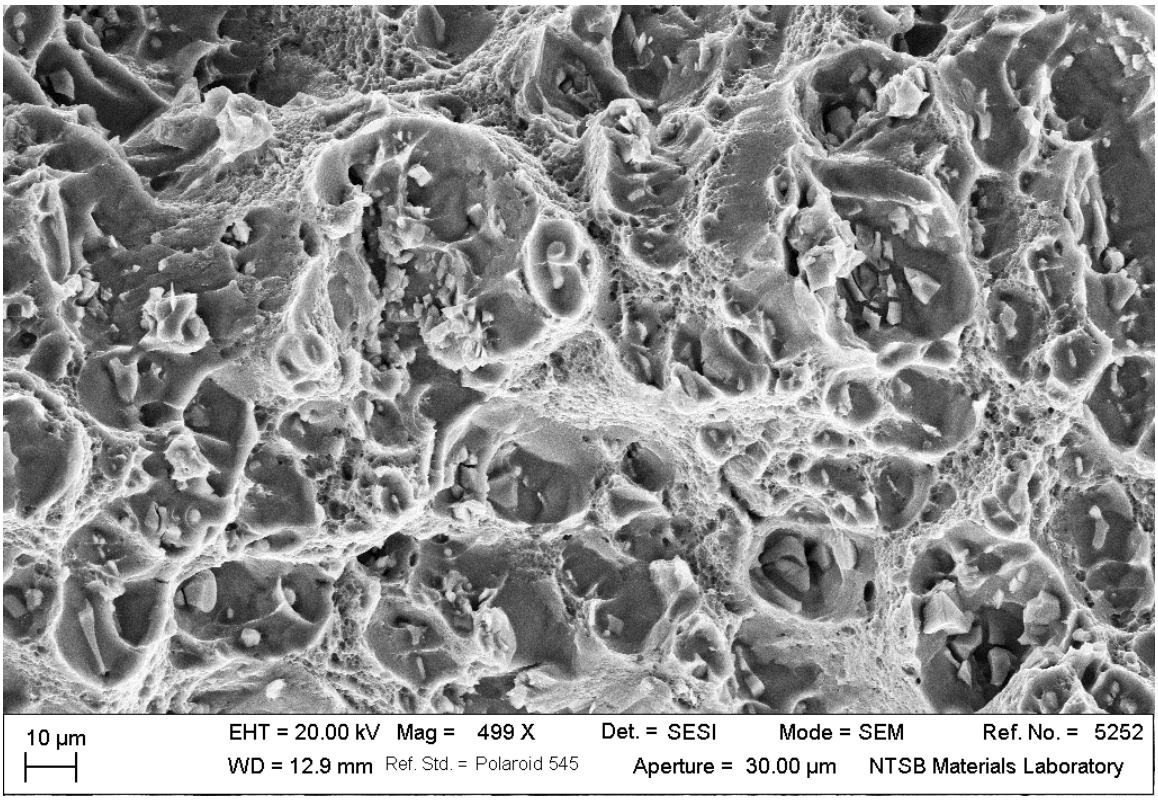

Figure 18 – SE micrograph of dimpled rupture on an area of the propeller material intentionally overstressed (lab opened).

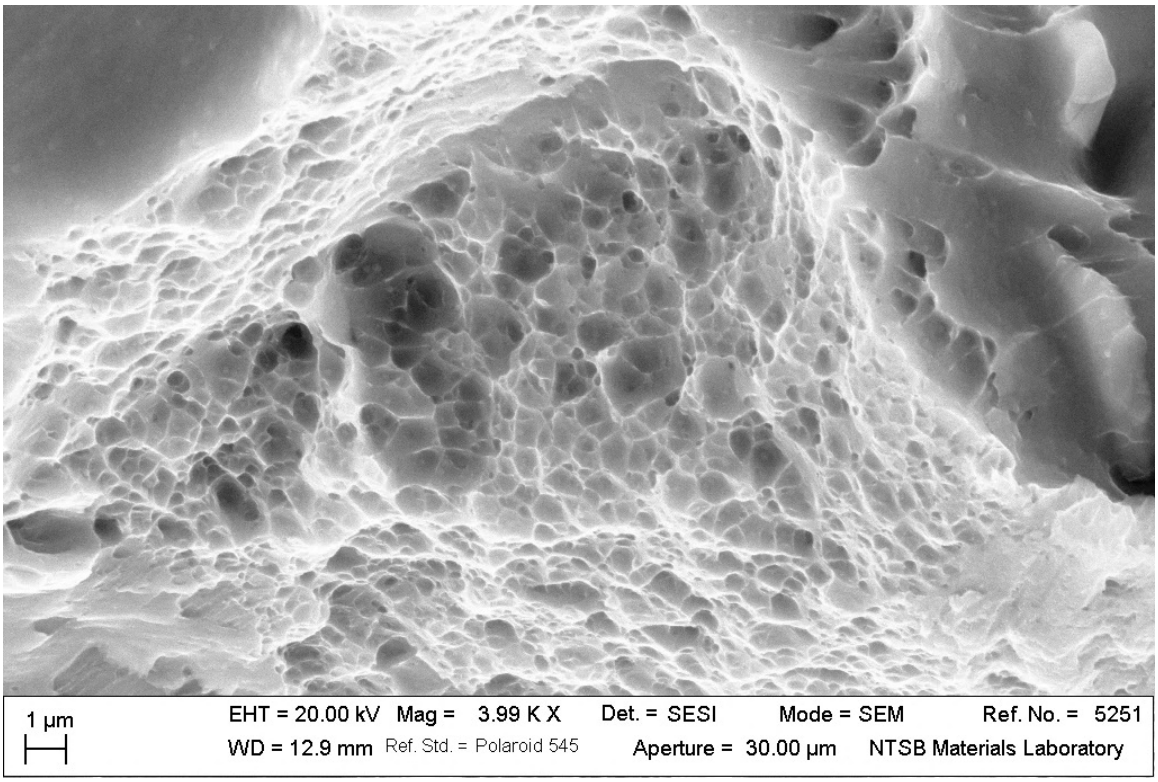

Figure 19 – SE micrograph of a closer view of the dimpled rupture in Figure 18.